Ship targets feature extraction with GNSS-based passive radar via ISAR approaches: preliminary experimental study

Federica Pieralice, DIET Dept. University of Rome "La Sapienza", federica.pieralice@uniroma1.it, Italy
Fabrizio Santi, DIET Dept. University of Rome "La Sapienza", fabrizio.santi@uniroma1.it, Italy
Debora Pastina, DIET Dept. University of Rome "La Sapienza", debora.pastina@uniroma1.it, Italy
Michail Antoniou, EESE Dept. University of Birmingham, m.antoniou@bham.ac.uk, UK
Mikhail Cherniakov, EESE Dept. University of Birmingham, m.cherniakov@bham.ac.uk, UK

Abstract

This paper focuses on a passive radar system based on Global Navigation Satellite Systems for maritime surveillance. While in the past the capability of this technology to detect ship targets at sea was proved, despite the low EIRP level of the GNSS, the objective of this paper is investigating the potential of the system to extract information concerning the detected target characteristics. An experimental study is here provided, showing that the Doppler gradient observed for ship targets of interest can be exploited making use of ISAR approaches for extracting ship features to be exploited in target recognition procedures.

1 Introduction

The monitoring of maritime traffic is important for both safety and security reasons. In fact, a large number of human activities takes place in the maritime domain, varying from cruise and trading ships up to vessels involved in nefarious activities such as piracy, human smuggling or terrorist actions. In this framework, the last years have seen an increasing research activity in radar sensors based on opportunistic sources for detecting and identifying ship targets at sea, motivated by the low-cost, license-free, silent and "green" operations allowed by the passive radar technology. Innovative solutions based on terrestrial transmitters such as DVB-T and GSM have been largely investigated and proven to be effective [1,2]: nevertheless, terrestrial-based passive radar cannot provide monitoring of areas such as the open sea. Our research focuses on Global Navigation Satellite Systems (GNSS): this is a prospective solution in the framework of maritime surveillance. Indeed, with their global coverage, GNSS are one of the few signal sources available both in coastal areas and in open sea. Moreover, they operate with large constellations, where 6-8 satellites of the single constellation are simultaneously illuminating the same area, so that up to 32 satellites could be exploited when all 4 GNSS systems (GPS, Galileo, Glonass, Beidou) will be operative offering the potentialities of waveform and spatial diversity with a single receiver.

In [3], the capability of a GNSS-based passive radar to detect ship targets has been assessed and experimentally verified using a large ferry (expected to provide a large radar cross section) at relatively short ranges (~2 Km). Moreover, in [4,5] long integration time techniques have been presented and shown being able to increase the detection performance of the system: the proper build-up of the received signal energy over long dwell (tens of seconds) has been shown being an effective solution to counteract the low

power budget provided by GNSS, which represents the main bottleneck of the system, allowing the detection of low observable targets. Techniques and results in [3-5] refer to the exploitation of single bistatic couples while the use of multiple transmitters has been considered in [6] for localization purposes and in [7] for the improvement of detection performance with respect to performance achievable in the single baseline case.

In this paper, the possibility to extract features of the detected targets is being investigated. Usually, after a target is detected, the radar user attempts to identify it by making use of automatic target recognition procedures, and this goal can be achieved by ship imagery obtained with the well-known principle of the Inverse Synthetic Aperture Radar (ISAR) [8]. With this objective in mind, as a first step we present in this work an experimental study aimed at showing that the Doppler gradient and the Doppler resolution observed by the GNSS-based passive radar over proper coherent processing intervals (CPIs) could suffice to roughly identify the dimensional class of the detected ship.

The paper is organized as follows: an overview of the GNSS-based passive radar is given in Section II; the extraction of the ship feature is described in Section III while Section IV shows the results achieved against real maritime datasets; conclusion is drawn in Section V.

2 System overview

The operative conditions are given by a GNSS transmitter (Tx) and a receiver (Rx) that can be mounted on the coast or on a moored buoy. The receiver is equipped with an antenna pointed toward the surveyed area and collecting the signal reflections (radar antenna) while a low-gain antenna pointed toward the sky records the direct signal for the synchronization (reference antenna), [3]. **Figure 1** shows the considered reference system: it is
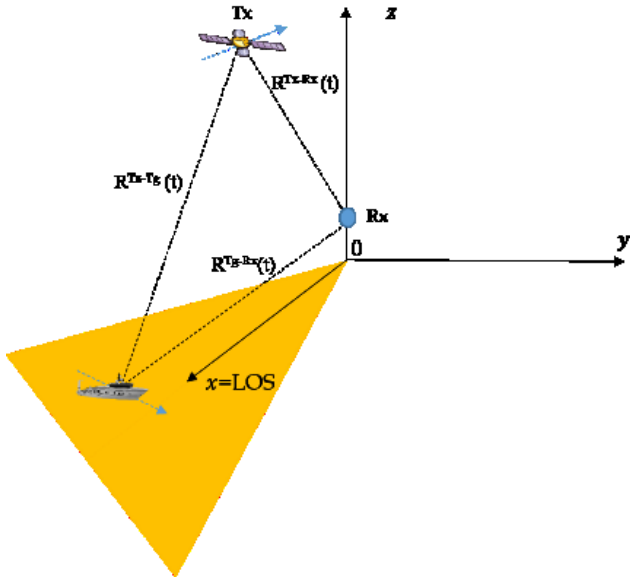
Figure 1: Local reference system.

a right-handed $(0, x, y, z)$ Cartesian plane, centred in the projection of the receiver position on the ground plane (x, y) and where the x-axis represents the projection of the radar antenna Line-Of-Sight (LOS) onto the local tangent plane to the Earth.

Let us consider a material point P moving in the field of view of the radar antenna, whose instantaneous position can be denoted as $P(t) = (x(t), y(t))$, being t the slow-time defined in the interval [-T/2,T/2] being T the overall observation time. This corresponds to a bistatic range history equal to

$$R(t) = R_{Tx-P}(t) + R_{P-Rx}(t) - R_{Tx-Rx}(t) \qquad (1)$$

where R_{Tx-P}, R_{P-Rx} and R_{Tx-Rx} are the instantaneous distances transmitter-to-point, point-to-receiver and transmitter-to-receiver, respectively. As commonly done in passive radar, in (1) the bistatic range is calculated taking into account the compensation of the baseline, since the range compressed data are obtained by the cross-correlation between the reflected signal and the reference signal (regenerated from the estimates of the direct signal delay, Doppler and phase) [3]. Let λ be the wavelength, the corresponding bistatic Doppler history is given by

$$f_d(t) = -\frac{1}{\lambda}\dot{R}(t) \qquad (2)$$

The main limitation of GNSS for detection purposes is the low level of e.m. field reaching the Earth' surface, [9]. While high-RCS targets can be detected by exploiting short coherent processing intervals (CPIs), in the order of 1-2 secs, the detection of low/medium RCS targets at longer ranges may require exploiting the signal reflections over integration times in the order of tens of seconds. This is achieved in turn by: i) segmenting T in shorter time intervals (frame) and achieving a sequence of single-frame RD maps; ii) compensating the target motion by making use of proper filter banks so that the same target is aligned on the same range&Doppler position in the sequence of RD maps; iii) non-coherently integrating the compensated RD maps over the selected observation time, [3-5].

Once the target has been detected, it can be of interest to extract some of its relevant features such as information about the target size: this could be obtained by properly exploiting the synthetic aperture provided by the target motion by means of ISAR techniques.

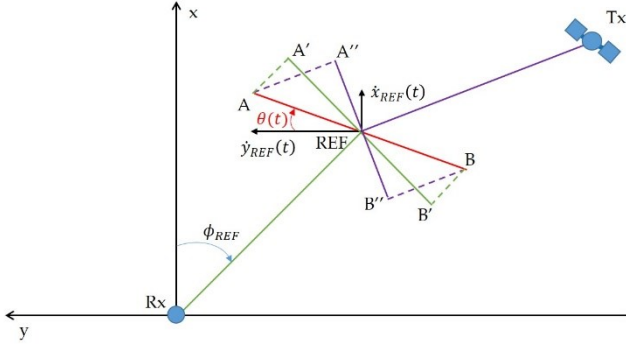# 3 Ship target instantaneous Doppler bandwidth

As usual in ISAR literature, the generic target motion can be decomposed as the translation of a reference point (fulcrum) and the rotation of the target around that point. While searching the ship, techniques [3-5] compensate the motion of the target fulcrum over consecutive frames. That is to say, they take into account the fulcrum trajectory $\{x_{REF}(t), y_{REF}(t)\}$. Therefore, the target fulcrum is imaged in the RD domain at a specific Doppler frequency that depends on the target kinematics at the reference time instant pertaining the overall integration window.

Since the target motion compensation procedures in [3-5] relocate the target energy over the same RD position, they, in principle, do not affect the imagery. Therefore, for ISAR purposes only and provided that a single frame suffices (high-RCS targets), we can consider the observation time limited to the CPI, namely the reference frame duration.

Let us consider the ship target characterized by point scatterers A and B identifying the edges of the target and following a trajectory characterized by the heading angle $\theta(t) = tg^{-1}[\dot{x}_{REF}(t)/\dot{y}_{REF}(t)]$ measured clockwise from y-axis and variable during the acquisition time, as is shown in **Figure 2**. Changes in the motion direction are taken into account by considering the target rotating at an angular velocity $\omega_{rot}(t) = \dot{\theta}(t)$ around a vertical rotation axis (i.e. rotation normal to the ground plane). The direction of arrival of the target relative to receiver is ϕ_{REF}, measured clockwise from the LOS. In such situation, the target instantaneous Doppler bandwidth B_d (defined as the range of Doppler frequency values pertaining to points from A to B) is composed by two contributions, one related to the receiver and the other one related to the transmitter.

With respect to the receiver, both rotational and translational motions are expected to contribute to B_d. By considering a ship target with length $\overline{AB} = L$ and scatterers A and B at distance L/2 from the target fulcrum (*REF* in **Figure 2**), the Rx-related instantaneous Doppler bandwidth due to target rotation can be written as:

$$B_{d,r}{}' = \frac{\overline{A'B'}\,\omega_{rot}^0}{\lambda} \qquad (3)$$

Figure 2: Top-view of local reference system.

Parameter	Value
Satellite	GSAT0201
Ranging code	PRN E18 (E5a-Q)
Bistatic angle	97° ~ 85°
Azimuth (relevant to North)	163.8° ~ 163.9°
Elevation (relevant to ref. antenna)	18.9° ~ 18.2°
Carrier frequency	1176.45 MHz
Sampling frequency	50 MHz
Duration of the acquisition	145 s
Equivalent pulse repetition interval	1 ms
Coherent processing interval	3 s

Table 1: Experimental and signal processing parameters

where $\omega_{rot}^0 = \dot{\theta}(0)$ is the angular velocity calculated at the image time $t = 0$ and $\overline{A'B'}$ is the projection of $\overline{AB}$ on the normal to the line joining the receiver and the target reference point. The Rx-related instantaneous Doppler bandwidth due to target translation can be proven being equal to:

$$B_{d,t} = -\left(\frac{1}{\lambda}\dot{R}_{B-Rx}(0) - \frac{1}{\lambda}\dot{R}_{A-Rx}(0)\right) =$$

$$= \frac{1}{\lambda}\left(\frac{x_A^0 \dot{x}_{REF}^0 + y_A^0 \dot{y}_{REF}^0}{R_{Rx-A}}\right) - \frac{1}{\lambda}\left(\frac{x_B^0 \dot{x}_{REF}^0 + y_B^0 \dot{y}_{REF}^0}{R_{Rx-B}}\right) \quad (4)$$

where x_A, y_A are the coordinates of the point A, x_B, y_B are the coordinates of the point B, R_{Rx-A} and R_{Rx-B} are the instantaneous distances transmitter-to-point A and B, respectively and the subscript 0 denotes the position at the image time.

Concerning the transmitter, due to the very large distance between the target and the transmitter, only the rotation motion contributes to instantaneous Doppler bandwidth, [10]. Similarly to eq. (3), this contribution can be evaluated as

$$B_{d,r}{''} = \frac{\overline{A''B''}\,\omega_{rot}^0 \cos\theta_{Tx}^0}{\lambda} \quad (5)$$

where $\overline{A''B''}$ is distance of the points A and B from the line joining the transmitter and the target reference point and θ_{Tx}^0 is the out-of-plane angle between the (x,y) plane and the satellite at the reference time $t = 0$. In eq. (5), the projection according to the θ_{Tx}^0 value allows considering the effective rotation rate with respect to the transmitter LOS, [8].

The total instantaneous Doppler bandwidth is the summation of the three components calculated above:

$$B_d = B_{d,t} + B_{d,r}{'} + B_{d,r}{'} \quad (6)$$

This Doppler bandwidth can be compared to the Doppler resolution (1/CPI) to obtain the number of Doppler resolution cells occupied by the target: potentialities for feature extraction arise when $B_d \gg 1/CPI$ so that different target scattering centers can be separated in the Doppler domain and therefore an image or at least a Doppler/cross-range profile is obtained, [11-12].

4 Experimental results

The potentialities for feature extraction approach are now demonstrated on an experimental dataset to verify its effectiveness. A maritime experimental campaign was conducted in the eastern coastal area of Plymouth harbor in UK and a Galileo satellite was exploited as illuminator of opportunity, as shown in **Figure 3** (a). The experimental receiver [**Figure 3** (b)] was equipped with two RF channels for recording direct and reflected signals, respectively. The target of opportunity was the commercial Brittany ferry shown in **Figure 3** (c), having length L = 184 m and width W = 25 m. The automatic identification system (AIS) information was recorded and used as ground truth to validate the experimental results. **Table 1** shows the experimental and signal processing parameters. This acquisition concerns a high size and high RCS target, therefore a short integration time suffices to detect it, [3].

Figure 4 shows the ideal target shape: for the purpose of this paper, it is assumed that it can be roughly represented by an L×W rectangle which orientation depends on the target heading at the time instant of interest.

Figure 5 shows the RD images achieved over a CPI of 3 s around two different reference time instants. Each image has been obtained by applying to the range compressed data a proper dechirping followed by a Fast Fourier Transform. In the images, 0 dB denotes the mean background power. The ship shape circumscribed to the ship deck is also shown: the four vertexes of the rectangle in Figure 4 have been projected on the RD plane ('*' black markers) evaluating their position on the (x, y) plane according to
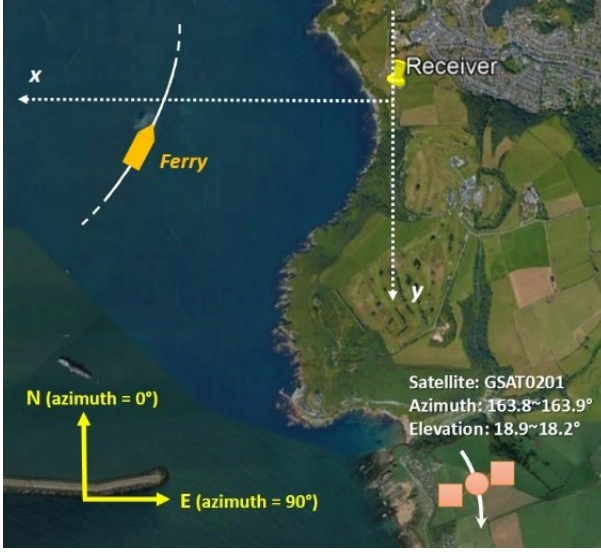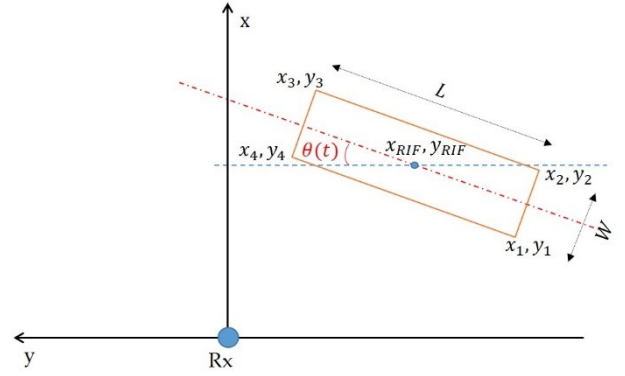
(a)
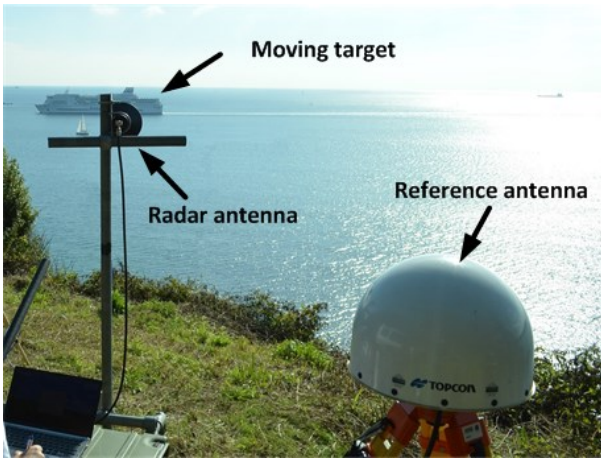
(b)

(c)

Figure 3: (a) Schematic diagram of the experimental GNSS-based radar data acquisition geometry, (b) the experimental setup of the receiving system and (c) the optical photograph of the ferry.

$$\begin{bmatrix} x_i(t) \\ y_i(t) \end{bmatrix} = \begin{bmatrix} \cos \omega_{rot} t & \sin \omega_{rot} t \\ -\sin \omega_{rot} t & \cos \omega_{rot} t \end{bmatrix} \begin{bmatrix} x_i^0 - x_{REF}^0 \\ y_i^0 - y_{REF}^0 \end{bmatrix} + \begin{bmatrix} x_{REF}(t) \\ y_{REF}(t) \end{bmatrix}, \quad i = 1 \dots 4 \quad (7)$$

Figure 4: Target silhouette.

where $\{x_{REF}(t), y_{REF}(t)\}$ and $\dot{\theta} = \omega_{rot}$ are retrieved from AIS data and using these coordinates inside eqs. (1-2).

For the considered case study, the overall bandwidth calculated with (6) is equal 3.2 Hz and 4.0 Hz with reference to Figure 5 (a) and (b), respectively. Therefore, the Doppler cells occupied by the target are 9.6 and 12, respectively. As evident, the area bounded by the projected rectangular shape fits well with the target dimension demonstrating the potentialities for feature extraction. Further, it is worth to explicitly note that the target size could be retrieved by properly scaling the Doppler frequency axis.

5 Conclusions

The GNSS-based passive radar is an emerging technology whose utilization in the maritime surveillance framework represents an innovative and prospective solution. Previous researches showed how the detection of vessels at sea is fundamentally possible with such a system. Now, this paper has investigated the possibility to extract features of the detected ships by exploiting the principle of the Inverse SAR.

The chance to extract useful information related to the target size depends on the number of Doppler cells over which the target instantaneous Doppler bandwidth spans. First, the instantaneous Doppler bandwidth provided by the detected ship has been evaluated as composed by three contributions: the receive related bandwidth due to target translation, the receiver related bandwidth due to target rotation and the satellite related bandwidth due to target rotation. Then, an experimental study has been carried out. The signal transmitted by a satellite of the Galileo constellation and reflected from a ferry has been collected over a dwell time of more than two minutes. By appropriate signal processing, the corresponding RD images over consecutive CPIs have been obtained, allowing the identification of the area occupied by the ferry. The obtained results showed that the ferry projected over the RD plane accordingly to the theoretical Doppler bandwidth evaluation is in good agreement with the target size that can be evaluated from the experimental images. . Moreover, it has been seen how the energy span over multiple resolution cells, thus proving that information about the size of the detected target can be retrieved and therefore exploited in ATR procedures
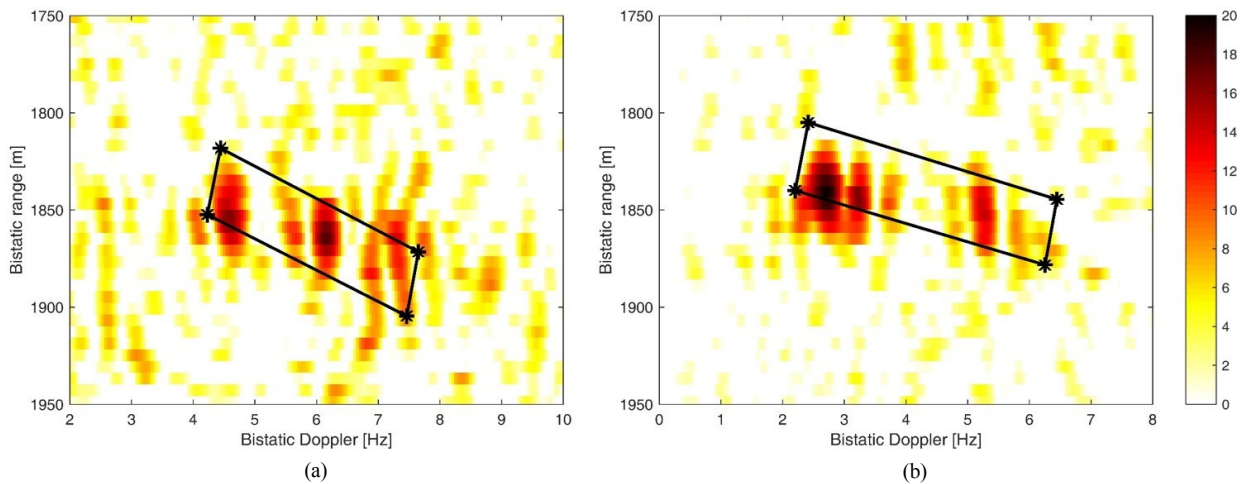
Figure 5: Calculated corner point superimposed on ship RD images obtained for two different reference time instants.

References

[1] T. Martelli, F. Colone, E. Tilli, A. Di Lallo, "Multi-frequency target detection techniques for DVB-T based passive radar sensors", (2016) *Sensors* (Switzerland), 16 (10), art. no. 1594.

[2] R. Zemmari, M. Broetje, G. Battistello, and U. Nickel, "GSM passive coherent location system: performance prediction and measurement evaluation," *IET Radar Sonar Navig.*, vol. 8, no. 2, pp. 94-105, 2014.

[3] H. Ma, M. Antoniou, D. Pastina, F. Santi, F. Pieralice, M. Bucciarelli, M. Cherniakov, "Maritime moving target indication using passive GNSS-based bistatic radar," *IEEE Transactions on Aerospace and Electronic Systems*, vol. 54, no. 1, pp. 115-130, Feb. 2018.

[4] F. Pieralice, F. Santi, D. Pastina, M. Bucciarelli, H. Ma, M. Antoniou, M. Cherniakov, "GNSS-Based Passive Radar for Maritime Surveillance: Long Integration Time MTI Technique," *IEEE Radar Conf.*, Seattle, USA, May 2017.

[5] F. Santi, D. Pastina, M. Bucciarelli, "Maritime moving target detection technique for passive bistatic radar with GNSS transmitters," *18th International Radar Symposium*, Prague, CZ, June 2017.

[6] H. Ma, D. Tzagkas, M. Antoniou, M. Cherniakov, "Maritime moving target indication and localization with GNSS-based multistatic radar: experimental proof of concept," *18th International Radar Symposium*, Prague, CZ, June 2017.

[7] F. Pieralice, D. Pastina, F. Santi, M. Bucciarelli, "Multi-transmitter ship target detection technique with GNSS-based passive radar," *International Conference on Radar Systems*, Belfast, UK, Oct. 2017.

[8] D.R. Wehner: 'High-resoultion radar' (Artech House, Boston, MA, USA, 1995, 2nd edn.), pp. 359–364.

[9] X. He, M. Cherniakov, T. Zeng., "Signal detectability in SS-BSAR with GNSS non-cooperative transmitter," *IEE Proceedings Radar, Sonar and Navigation*, vol. 152, no. 3, pp. 124-132, Jun. 2005.

[10] D. Pastina, D. Cristallini, "Passive bistatic ISAR based on geostationary satellites for coastal surveillance," *2010 IEEE Radar Conference*, Washington (USA), May 2010.

[11] D. Pastina, , F. Colone, , T. Martelli, , P. Falcone, , "Parasitic exploitation of Wi-Fi signals for indoor radar surveillance", *IEEE Transactions on Vehicular Technology*, vol. 64, no. 4, pp. 1401-1415, Apr. 2015..

[12] F. Colone, , D. Pastina, , V. Marongiu, , "VHF Cross-Range Profiling of Aerial Targets Via Passive ISAR," *IEEE Transactions on Aerospace and Electronic Systems*, vol. 53, no. 1, pp. 218-235, Feb. 2017.